Supplementary Information for

A Conceptual Translation of Homogeneous Catalysis into Heterogeneous Catalysis: Homogeneous-Like Heterogeneous Gold Nanoparticle Catalyst Induced by Ceria Supporter

Zhen-Xing Li,[a] Wei Xue,[a,c] Bing-Tao Guan,[b] Fu-Bo Shi,[a] Zhang-Jie Shi*[b] Hong Jiang*[a,c] and Chun-Hua Yan*[a]

[a] Beijing National Laboratory for Molecular Sciences, State Key Laboratory of Rare Earth Materials Chemistry and Applications, PKU-HKU Joint Laboratory on Rare Earth Materials and Bioinorganic Chemistry, Peking University, Beijing 100871, China.

[b] Key Laboratory of Bioorganic Chemistry and Molecular Engineering of Ministry of Education, College of Chemistry and Molecular Engineering, Peking University, Beijing 100871, China.

[c] Institute of Theoretical and Computational Chemistry, Peking University, Beijing 100871, China.

* To whom correspondence should be addressed. E-mail: yan@pku.edu.cn (C.H.Y.); zshi@pku.edu.cn (Z.J.S.); h.jiang@pku.edu.cn (H.J.)

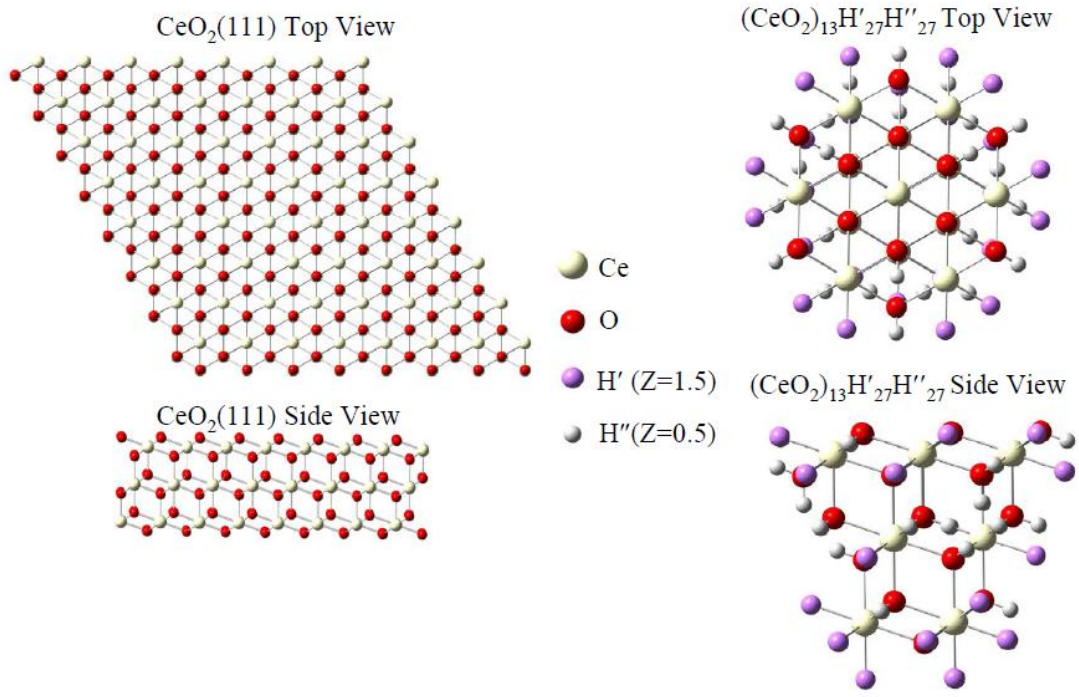

Figure S1. To mimic the properties of $CeO_2(111)$ surface using $(CeO_2)_{13}H'_{27}H''_{27}$ cluster model, in which H′ and H″ are the pseudo-hydrogens with the corresponding fractional charge in parentheses.

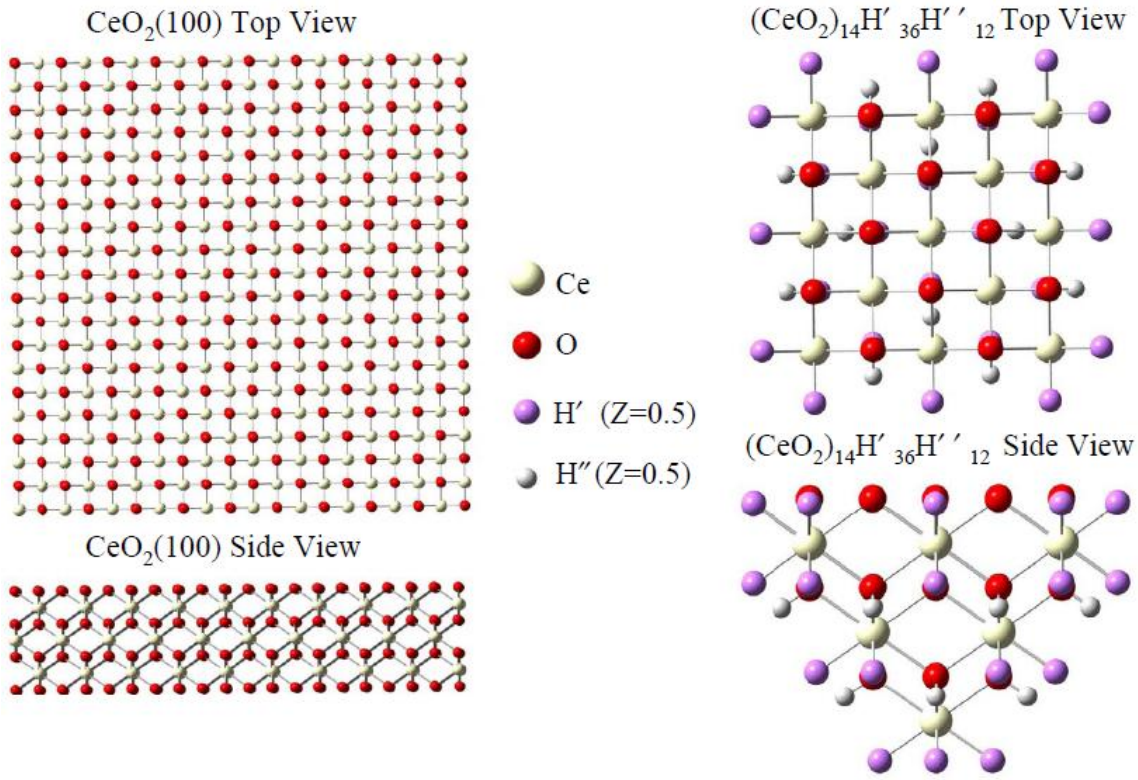

Figure S2. $(CeO_2)_{14}H'_{36}H''_{12}$ cluster model mimicking $CeO_2(100)$ surface.

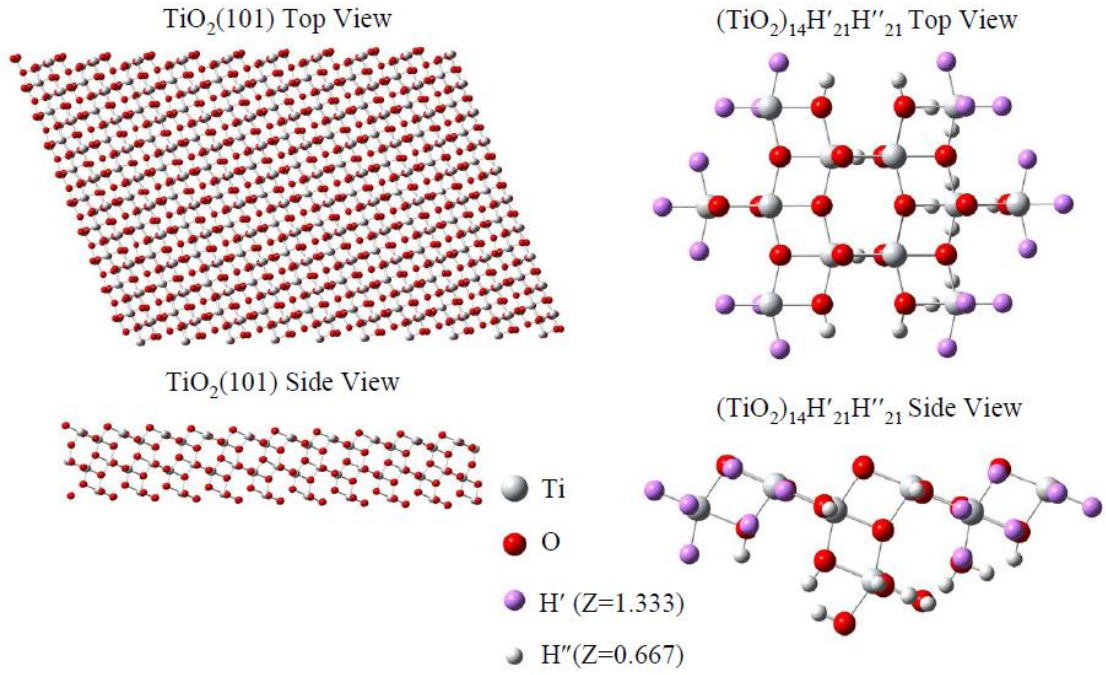

Figure S3. $(TiO_2)_{14}H'_{21}H''_{21}$ cluster model mimicking anatase(101) surface.

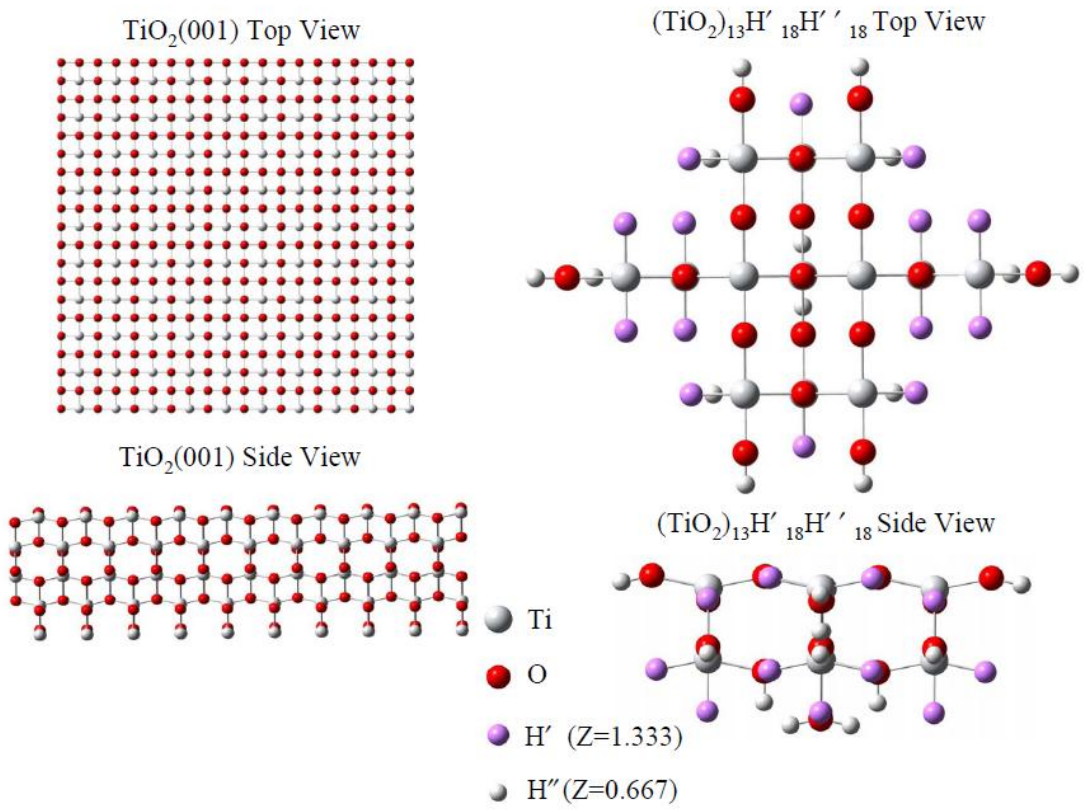

Figure S4. $(TiO_2)_{13}H'_{18}H''_{18}$ cluster model mimicking anatase(001) surface.

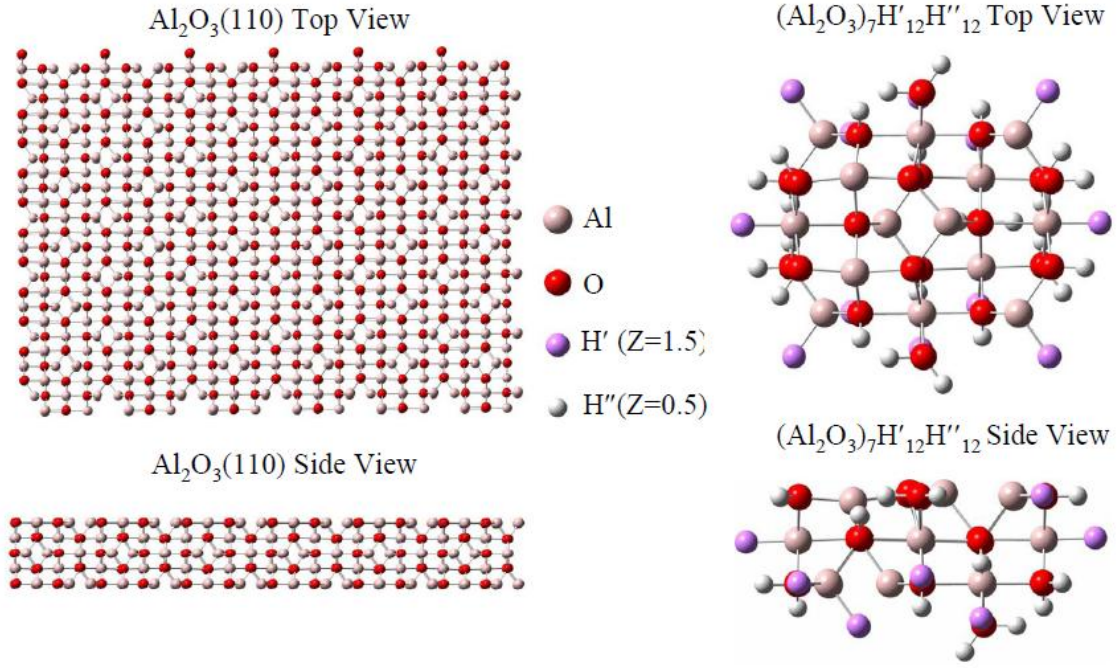

Figure S5. $(Al_2O_3)_7H'_{12}H''_{12}$ cluster model mimicking γ-Al_2O_3(110) surface.

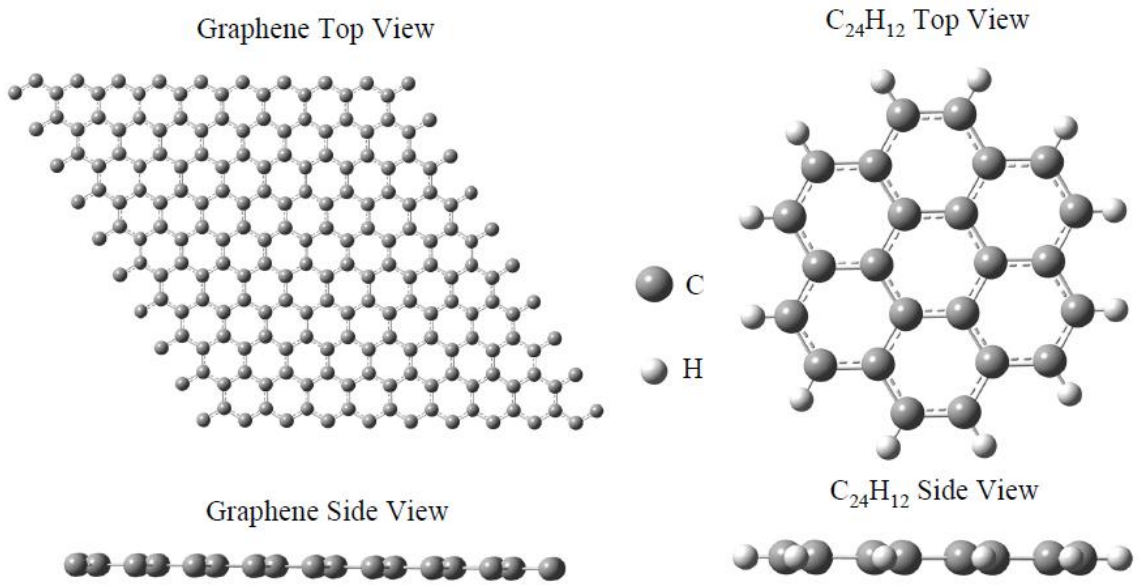

Figure S6. $C_{24}H_{12}$ cluster model mimicking graphene.

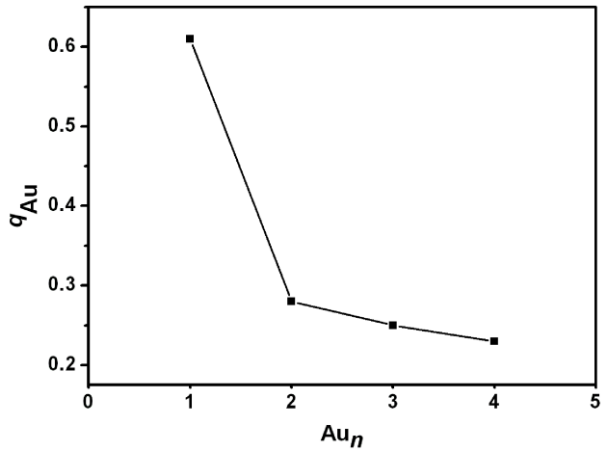

Figure S7. The average charge state of gold atom in Au_n (n = 2 – 4) clusters on $(CeO_2)_{14}H'_{36}H''_{12}$ cluster.

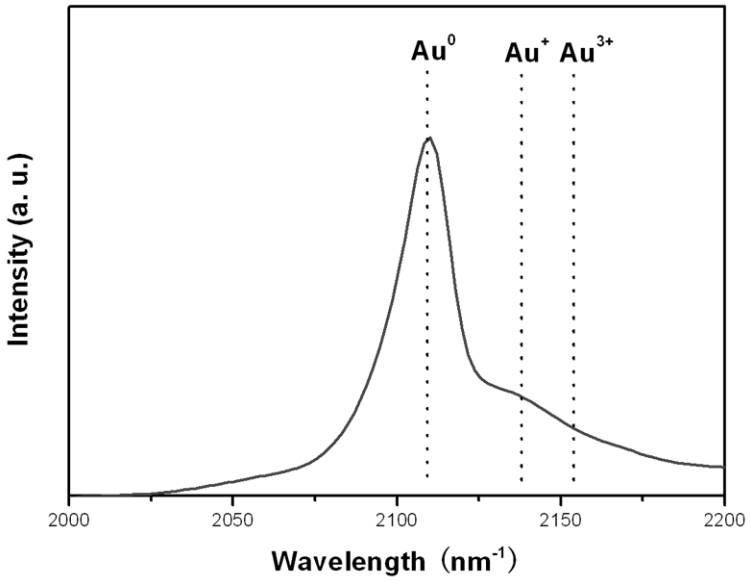

Figure S8. FTIR spectra of CO adsorbed on gold supported on CeO_2 nanocube at a CO pressure of 30 Torr and at room temperature.

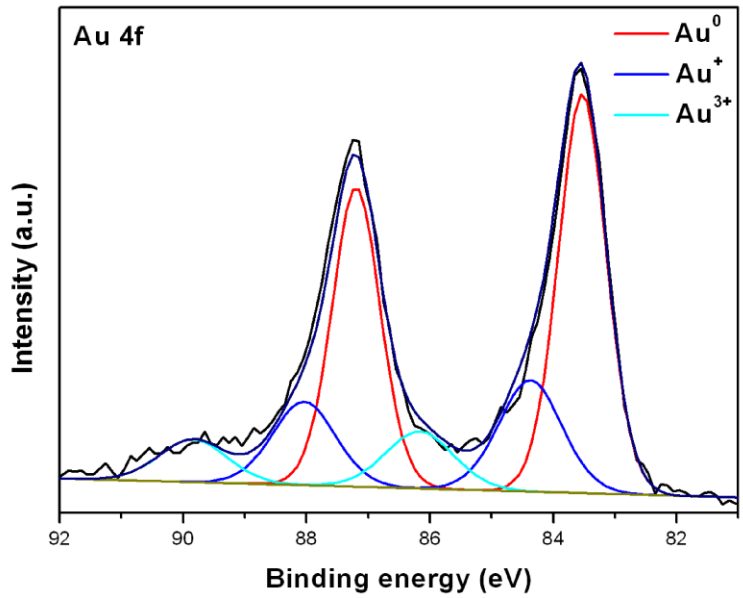

Figure S9. X-ray photoelectron spectroscopic scan survey in the region of Au 4d of gold supported on CeO_2 nanocube.

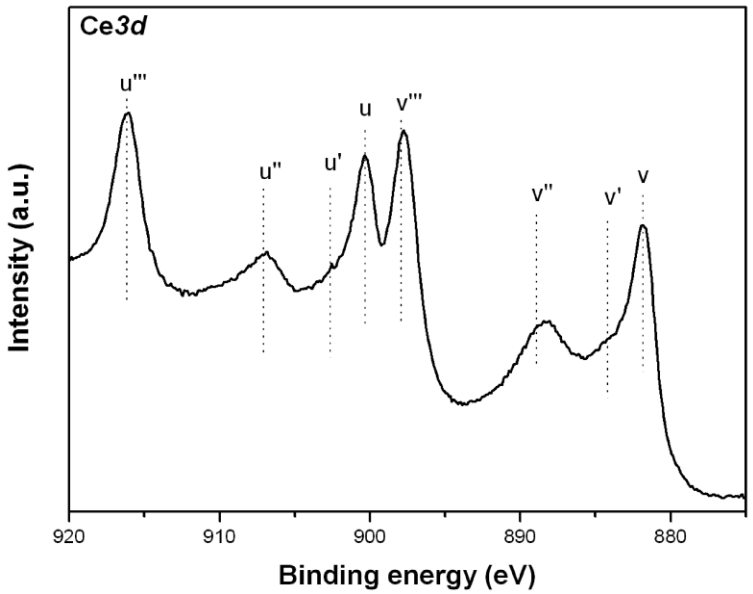

Figure S10. X-ray photoelectron spectroscopic scan survey in the region of Ce 3d of gold supported on CeO_2 nanocube.

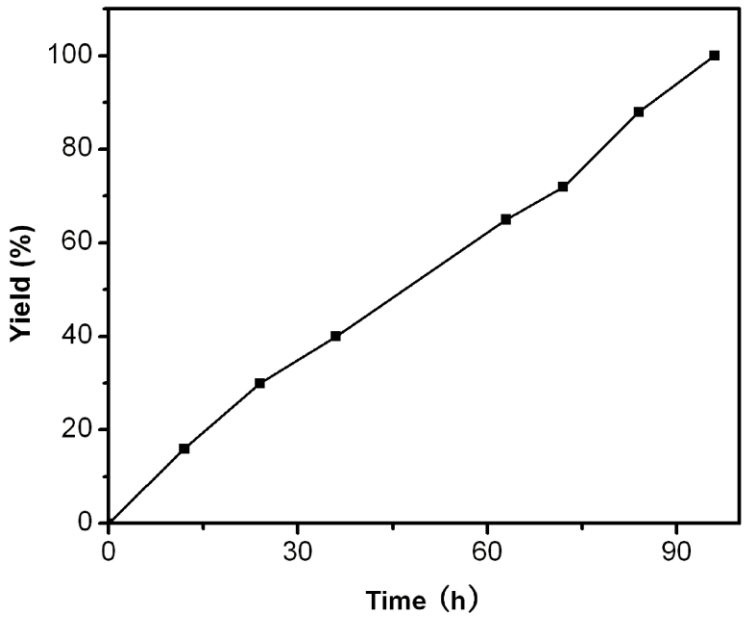

Figure S11. The reaction yield as a function of time for Au/CeO_2 nanocube catalysts.

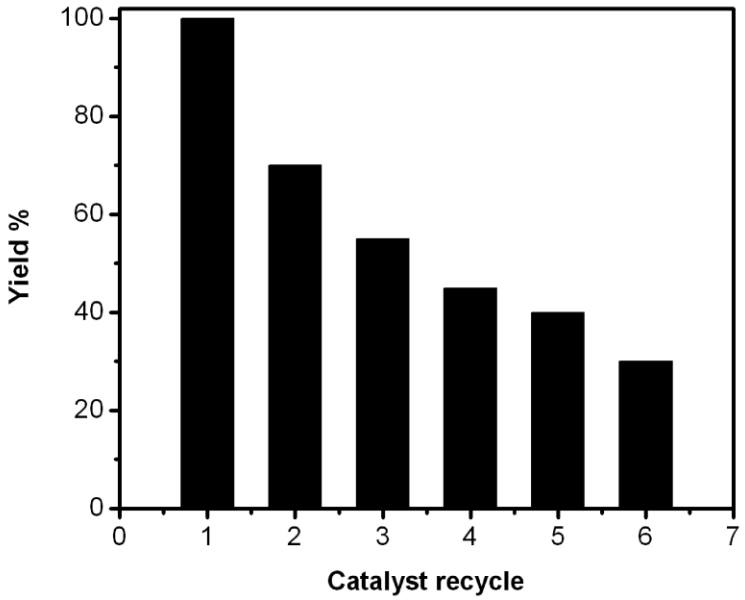

Figure S12. Au/CeO_2 nanocube catalysts for cycloisomerizations of enynes after different uses.

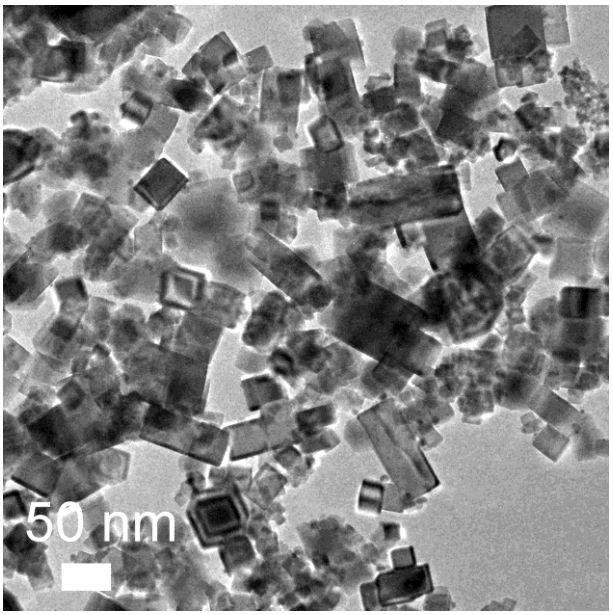

Figure S13. Transmission electron microscope (TEM) images of Au/CeO_2 nanocubes after the reaction. No leaching or aggregation is observed.

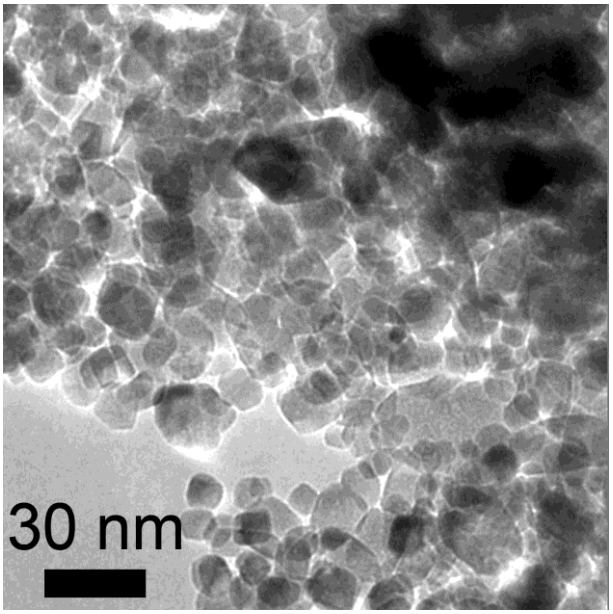

Figure S14. Transmission electron microscope (TEM) images of Au/TiO_2 nanoparticles.

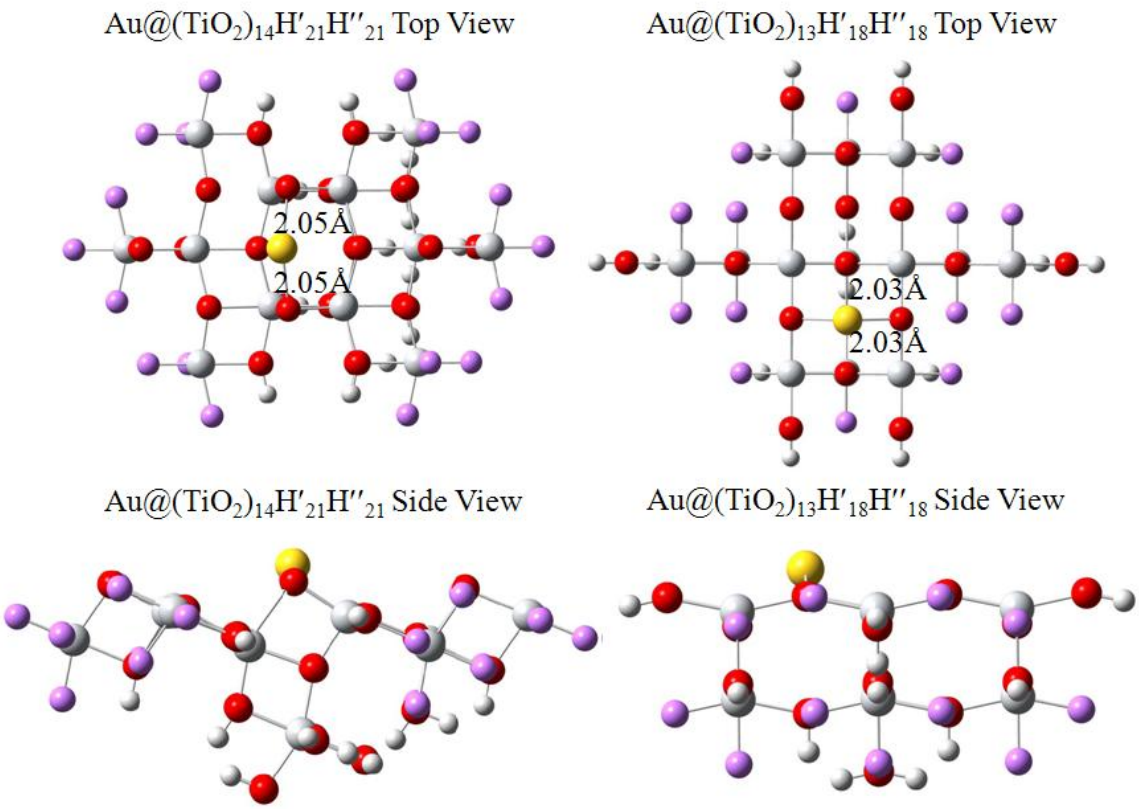

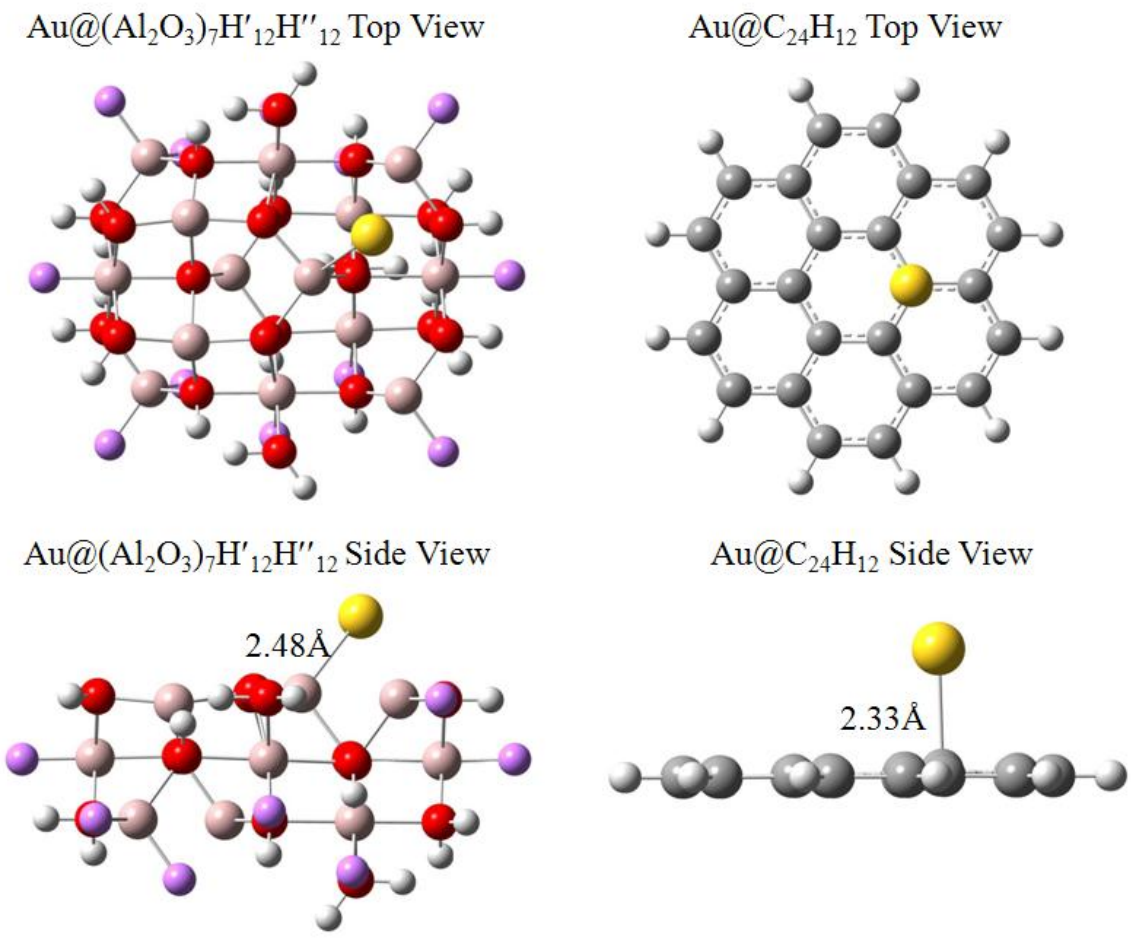

Figure S15. Calculated structures of a Au adsorption at TiO_2(101), TiO_2(001), γ-Al_2O_3(110) and the surface of monolayer GP.

Table S1 The chemisorption energies of carbon monoxide on $(CeO_2)_{13}H'_{27}H''_{27}$ cluster, comparing to the data in the references.

Model	Method	Site	*r*(C-Ce)/Å	E_{ads}/eV	Reference
Slab	PW91	atop Ce	2.86	-0.17	Yang, Z. et al. *Chem. Phys. Lett.* **2004**, *396*, 384.
Slab	PW91+U	atop Ce	2.86	-0.26	Nolan, M. et al. *Surf. Sci.* **2006**, *600*, L175.
Slab	PW91+U	atop Ce	2.88	-0.26	Nolan, M. et al. *J. Phys. Chem. B* **2006**, *110*, 16600.
Slab	PBE+U	atop Ce	2.86	-0.17	Huang, M. et al. *J. Phys. Chem. C* **2008**, *112*, 8643.
Slab	PW91+U	atop Ce	2.91	-0.18	Jiang, S. Y. et al. *Acta Phys. -Chim. Sin.* **2009**, *25*, 1629.
Embedded Cluster	LDA	atop Ce	2.856	-0.54	Müller, C. et al. *Surf. Sci.* **2009**, *603*, 2619.
	Exp.			~-0.2	Zaki, M. et al. *Spectrochim. Acta* **1987**, *43A*, 1455.
Saturated Cluster	LDA	atop Ce	2.73	-0.46	This work

Table S2 The vibrations of carbon monoxide on $(CeO_2)_{13}H'_{27}H''_{27}$ cluster, comparing to the data in the references.

Model	Method	Site	ν(C-O)$_{model}$/cm^{-1}	ν(C-O)$_{gas}$/cm^{-1}	Reference
	Exp.			2143	Street, S.C. et al. *Ann. Rev. Phys. Chem.* **1997**, *48*, 43.
	Exp.			2148	Reinhardt, P. A. et al. *Phys. Rev. B* **1996**, *54*, 14812.
	Exp.		2165		Bensalem, A. et al. *Appl. Catal. A-Gen.* **1995**, *121*, 81.
	Exp.		2177		Li, C. et al. *J. Chem. Soc. Faraday Trans.* **1989**, *185*, 929.
Slab	PW91	atop Ce	2082	2076	Yang, Z. et al. *Chem. Phys. Lett.* **2004**, *396*, 384.
Slab	PW91+U	atop Ce	2128	2103	Nolan, M. et al. *Surf. Sci.* **2006**, *600*, L175.
Saturated Cluster	LDA	atop Ce	2127	2124	This work

Table S3. The state of charge of gold atom on $(CeO_2)_{13}H'_{27}H''_{27}$ cluster.

Model	Method	Site	q_{Au}	E_{ads}/eV	Reference
Slab	PW91+U	bridge O	+0.33	-1.15	Hernandez, N. C. et al. *Phys. Chem. Chem. Phys.* **2009**, *11*, 5246.
Slab	PW91+U	bridge O	+0.32	-1.17	Zhang, C. J. et al. *J. Chem. Phys.* **2008**, *129*, 194708.
Slab	PBE	atop O	+0.35	-1.26	Liu, Z. P. et al. *Phys. Rev. Lett.* **2005**, *94*, 196102.
Saturated Cluster	LDA	atop O	+0.28	-1.44	This work

Table. S4. Gold loading and XPS Au4f peak analyses for Au on CeO_2, TiO_2, Al_2O_3, C and grapheme.

Entry	**Catalyst**	**Au (wt %)**	**XPS Au4f peak**		
			Au^0	**Au^+**	**Au^{3+}**
1	Au/CeO_2	1.1	64%	23%	13%
2	Au/TiO_2	1.3	73%	14%	13%
3	Au/Al_2O_3	1.2	83%	9%	8%
4	Au/C	0.9	85%	10%	5%
5	Au/GP	0.9	100%	—	—

Table S5. The charge state distribution of gold atom on the CeO_2 (100), TiO_2(101), TiO_2(001), γ-Al_2O_3(110) and the surface of monolayer GP.

Support	**Model**	**Site**	**r(Au-O/Al/C)/Å**	**q_{Au}**
CeO_2 (100)	$(CeO_2)_{14}H'_{36}H''_{12}$	hollow O	1.95	+0.61
TiO_2 (101)	$(TiO_2)_{14}H'_{21}H''_{21}$	bridge O	2.05	+0.32
TiO_2(001)	$(TiO_2)_{13}H'_{18}H''_{18}$	bridge O	2.03	+0.31
Al_2O_3 (110)	$(Al_2O_3)_7H'_{12}H''_{12}$	atop Al	2.48	+0.10
GP	$C_{24}H_{12}$	atop C	2.33	+0.03